Diiron Thiadithiolates as Active Site Models for the Iron-Only Hydrogenases: Synthesis, Structures, and Catalytic H_2 Production

Li-Cheng Song,* Zhi-Yong Yang, Yu-Juan Hua, Hu-Ting Wang, Yang Liu, and Qing-Mei Hu

Department of Chemistry, State Key Laboratory of Elemento-Organic Chemistry, Nankai University, Tianjin 300071, People's Republic of China

Received December 29, 2006

The first diiron thiadithiolates as active site models for the Fe-only hydrogenases were prepared. Treatment of $Fe_3(CO)_{12}$ with excess 1,2,4-trithiolane in THF at reflux afforded parent model $Fe_2(\mu\text{-}SCH_2)_2S(CO)_6$ (**1**) in 42% yield. Further treatment of **1** with $Cp(CO)_2Fe(BF_4)$ prepared in situ from $Cp(CO)_2FeI$ and $AgBF_4$ in CH_2Cl_2 gave cationic model $[Fe_2(\mu\text{-}SCH_2)_2S(CO)_6][Cp(CO)_2Fe](BF_4)$ (**2**) in 81% yield, while treatment of **1** with 2 equiv of Et_4NCN in MeCN or with *t*-BuNC in CH_2Cl_2 produced models $(Et_4N)_2[Fe_2(\mu\text{-}SCH_2)_2S(CO)_4(CN)_2]$ (**3**) and $Fe_2(\mu\text{-}SCH_2)_2S(CO)_4(t\text{-}BuNC)_2$ (**4**) in 93% and 51% yields, respectively. All the new models **1**−**4** were characterized by elemental analysis and spectroscopy, as well as by X-ray crystallography for **1**, **2**, and **4**. Furthermore, model **1** has been proved to be a catalyst for proton reduction of a weak acid Et_3NHCl to give hydrogen under electrochemical conditions.

Introduction

Fe-only hydrogenases are a class of enzymes that can catalyze hydrogen metabolism in many microorganisms.[1] The crystallographic studies on Fe-only hydrogenases CpI[2] and DdH[3] have indicated that the active site of Fe-only hydrogenases, the so-called H-cluster, is composed of a conventional cube-shaped 4Fe4S cluster bridged by a cysteine-S atom to the diiron subsite bearing three unusual ligands: CO, cyanide, and an organic dithiolate cofactor. To date, numerous model compounds have been synthesized and structurally characterized, such as those of diiron propanedithiolate (PDT) derivatives,[4] diiron azadithiolate (ADT) derivatives,[5] and diiron oxadithiolate (ODT) derivatives;[6] in addition, some of the reported models have been found to be catalysts for H/D exchange[7] or proton reduction to hydrogen.[8] We are interested in making model compounds in which a heteroatom is located in the middle of their dithiolate cofactors. This is because the N heteroatom in ADT (SCH_2NHCH_2S) cofactor has been suggested to play an essential role in the heterolytic cleavage of H_2 or H_2 evolution occurring in natural enzymes.[9] To explore the influence of such heteroatoms upon structure and properties of the artificial models and gain insight into the active site of Fe-only hydrogenases, we recently launched a study concerning a new type of model compounds that contain a thiadithiolate (TDT, SCH_2SCH_2S) cofactor in

Scheme 1

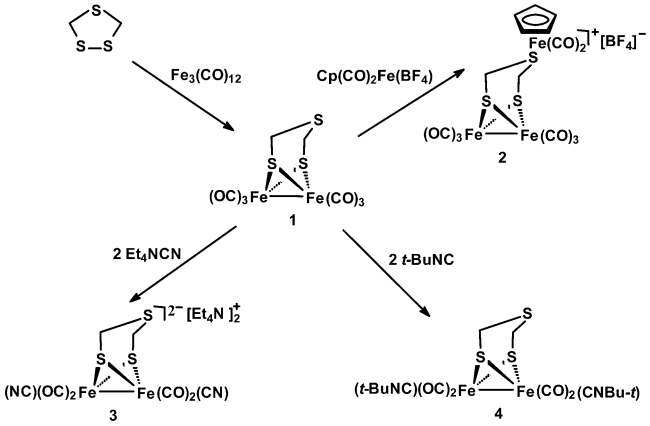

* To whom correspondence should be addressed. Fax: 0086-22-23504853. E-mail: lcsong@nankai.edu.cn.

(1) (a) Adams, M. W. W.; Stiefel, E. I. *Science* **1998**, *282*, 1842. (b) Cammack, R. *Nature* **1999**, *397*, 214. (c) Darensbourg, M. Y.; Lyon, E. J.; Zhao, X.; Georgakaki, I. P. *Proc. Natl. Acad. Sci. U.S.A.* **2003**, *100*, 3683. (d) Evans, D. J.; Pickett, C. J. *Chem. Soc. Rev.* **2003**, *32*, 268. (e) Alper, J. *Science* **2003**, *299*, 1686.

(2) Peters, J. W.; Lanzilotta, W. N.; Lemon, B. J.; Seefeldt, L. C. *Science* **1998**, *282*, 1853.

(3) Nicolet, Y.; Piras, C.; Legrand, P.; Hatchikian, C. E.; Fontecilla-Camps, J. C. *Structure* **1999**, *7*, 13.

(4) (a) Gloaguen, F.; Lawrence, J. D.; Schmidt, M.; Wilson, S. R.; Rauchfuss, T. B. *J. Am. Chem. Soc.* **2001**, *123*, 12518. (b) Lyon, E. J.; Georgakaki, I. P.; Reibenspies, J. H.; Darensbourg, M. Y. *J. Am. Chem. Soc.* **2001**, *123*, 3268. (c) Razavet, M.; Davies, S. C.; Hughes, D. L.; Barclay, J. E.; Evans, D. J.; Fairhurst, S. A.; Liu, X.; Pickett, C. J. *Dalton Trans.* **2003**, 586. (d) Tard, C.; Liu, X.; Ibrahim, S. K.; Bruschi, M.; De, Giola, L.; Davies, S. C.; Yang, X.; Wang, L.-S.; Sawers, G.; Pickett, C. J. *Nature* **2005**, *433*, 610. (e) Song, L.-C.; Cheng, J.; Yan, J.; Wang, H.-T.; Liu, X.-F.; Hu, Q.-M. *Organometallics* **2006**, *25*, 1544.

(5) (a) Lawrence, J. D.; Li, H.; Rauchfuss, T. B.; Bénard, M.; Rohmer, M.-M. *Angew. Chem., Int. Ed.* **2001**, *40*, 1768. (b) Li, H.; Rauchfuss, T. B. *J. Am. Chem. Soc.* **2002**, *124*, 726. (c) Song, L.-C.; Tang, M.-Y.; Su, F.-H.; Hu, Q.-M. *Angew. Chem., Int. Ed.* **2006**, *45*, 1130.

(6) (a) Song, L.-C.; Yang, Z.-Y.; Bian, H.-Z.; Hu, Q.-M. *Organometallics* **2004**, *23*, 3082. (b) Song, L.-C.; Yang, Z.-Y.; Bian, H.-Z.; Liu, Y.; Wang, H.-T.; Liu, X.-F.; Hu, Q.-M. *Organometallics* **2005**, *24*, 6126.

(7) (a) Zhao, X.; Georgakaki, I. P.; Miller, M. L.; Mejia-Rodriguez, R.; Chiang, C.-Y.; Darensbourg, M. Y. *Inorg. Chem.* **2002**, *41*, 3917. (b) Nehring, J. L.; Heinekey, D. M. *Inorg. Chem.* **2003**, *42*, 4288.

(8) (a) Gloaguen, F.; Lawrence, J. D.; Rauchfuss, T. B. *J. Am. Chem. Soc.* **2001**, *123*, 9476. (b) Chong, D.; Georgakaki, I. P.; Mejia-Rodriguez, R.; Sanabria-Chinchilla, J.; Soriaga, M. P.; Darensbourg, M. Y. *Dalton Trans.* **2003**, 4158.

(9) (a) Fan, H.-J.; Hall, M. B. *J. Am. Chem. Soc.* **2001**, *123*, 3828. (b) Nicolet, Y.; Lacey, A. L.; Vernède, X.; Fernandez, V. M.; Hatchikian, E. C.; Fontecilla-Camps, J. C. *J. Am. Chem. Soc.* **2001**, *123*, 1596. (c) Nicolet, Y.; Lemon, B. J.; Fontecilla-Caps, J. C.; Peters, J. W. *Trends Biochem. Sci.* **2000**, *25*, 138.

10.1021/om061186z CCC: $37.00
Publication on Web 03/06/2007

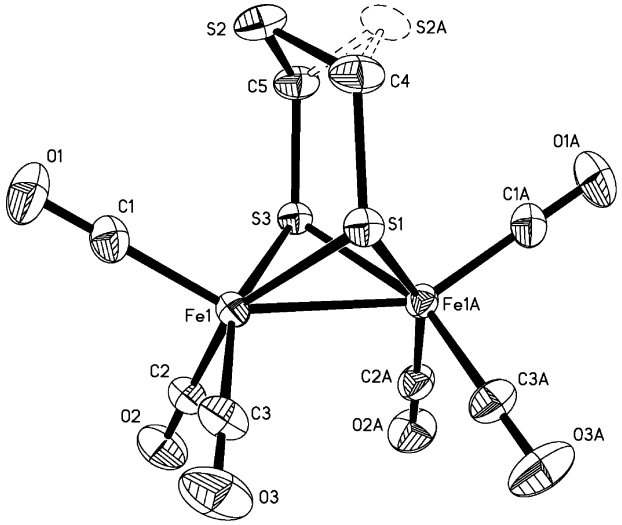

Figure 1. Molecular structure of **1** with 30% probability level ellipsoids.

Table 1. Selected Bond Lengths (Å) and Angles (deg) for 1

Fe(1)−C(1)	1.795(2)	Fe(1)−S(3)	2.2583(8)
Fe(1)−S(1)	2.2546(8)	S(2)−C(5)	1.727(3)
Fe(1)−Fe(1A)	2.5159(11)	S(2)−C(4)	1.745(3)
S(1)−C(4)	1.829(3)	S(3)−C(5)	1.832(3)
S(1)−Fe(1)−Fe(1A)	56.085(17)	Fe(1)−S(1)−Fe(1A)	67.83(3)
S(2)−C(4)−S(1)	118.83(16)	C(5)−S(2)−C(4)	102.18(14)
S(3)−Fe(1)−Fe(1A)	56.148(17)	C(5)−S(3)−Fe(1)	112.84(9)
C(4)−S(1)−Fe(1)	113.63(9)	Fe(1A)−S(3)−Fe(1)	67.70(3)

which the heteroatom S is located in middle position of the cofactor. Herein we report the synthesis, structures, and some properties of this new type of model compounds.

Results and Discussion

Synthesis and Characterization of Parent Model 1. Treatment of $Fe_3(CO)_{12}$ with 1,2,4-trithiolane, $(SCH_2)_2S$, in THF at reflux resulted in formation of the simplest TDT-type model, $Fe_2(\mu\text{-}SCH_2)_2S(CO)_6$ (**1**), in 42% yield (Scheme 1). Model **1** is an air-stable solid; even in solution it remains unchanged for several hours. Model **1** has been fully characterized by elemental analysis, spectroscopy, and X-ray crystallography. The IR spectrum of **1** displays four absorption bands in the range 2075−1990 cm^{-1} for its terminal carbonyls, whereas the ^1H NMR spectrum exhibits one singlet at 3.21 ppm attributed to its CH_2 groups. The X-ray crystallographic study of **1** (Figure 1 and Table 1) has revealed the structural similarity to its ODT and ADT analogues $Fe_2(\mu\text{-}SCH_2)_2O(CO)_6$[6] and $Fe_2(\mu\text{-}SCH_2)_2NMe(CO)_6$.[5a] In the crystal structure of **1** the middle sulfur atom in cofactor TDT is disordered with 50% S2 and 50% S2A to form two sets of two six-membered rings: Fe1−S1−C4−S2-C5−S3 (or Fe1A−S1−C4−S2A−C5−S3) in a boat-shaped conformation and Fe1A−S1−C4−S2−C5−S3 (or Fe1−S1−C4−S2A−C5−S3) in a chair-shaped conformation, respectively. All the Fe atoms in **1** adopt a distorted square pyramidal geometry with each Fe atom being displaced by about 0.39 Å from the pyramidal base toward the apical direction. In addition, the Fe−Fe bond length is 2.5159(11) Å, about 0.1 Å shorter than those reported for the oxidized state diiron subsite in the enzyme structures (2.62 and 2.60 Å)[2,3] and only 0.03 Å shorter than that in the reduced state diiron subsite of the enzyme structure (2.55 Å).[9b]

Synthesis and Characterization of Models 2−4. To show the coordinating ability of the middle S heteroatom in the TDT ligand of **1**, we further treated ca. 1 equiv of **1** with $Cp(CO)_2Fe(BF_4)$ (prepared in situ from $Cp(CO)_2FeI$ and $AgBF_4$)[10] in CH_2Cl_2 at room temperature; as a result, the expected cationic TDT-type model $[Fe_2(\mu\text{-}SCH_2)_2S(CO)_6][Cp(CO)_2Fe](BF_4)$ (**2**) was produced in 81% yield (Scheme 1). Similar to **1**, model **2** is an air-stable solid, but slightly air-sensitive in solution. Model **2** has also been characterized by elemental analysis, spectroscopy, and X-ray crystallography. The IR spectrum of **2** displays four absorption bands in the region 2085−2010 cm^{-1} for its terminal carbonyls. These bands are shifted toward higher frequencies relative to those of its parent complex **1**, obviously due to the decreased π-back-bonding from Fe atoms to their attached terminal carbonyls in the cationic portion of model **2**. The ^1H NMR spectrum of **2** exhibits two broad singlets at 3.51 and 4.05 ppm for its CH_2 groups. This indicates that the middle sulfur atom in the TDT cofactor of **2** has been fixed by the $Cp(CO)_2Fe$ moiety in cationic model **2**. That is, the interconversion between the two fused six-membered rings FeSCSCS in the TDT-bridged diiron moiety of model **2** becomes much slower to allow distinguishing the two diastereotopic hydrogen atoms in the CH_2 groups of model **2**. In addition, the ^{19}F NMR spectrum of **2** shows one singlet at −152.09 ppm attributed to its BF_4^- anions.[11]

Crystallographic analysis of **2** (Figure 2 and Table 2) has demonstrated that the middle sulfur atom in its TDT cofactor is indeed coordinated with the Fe atom of the $Cp(CO)_2Fe$ unit via the common equatorial bond of the boat- and chair-shaped six-membered rings Fe3−S2−C9−S1−C10−S3 and Fe2−S2−C9−S1−C10−S3. This is obviously in order to avoid the strong

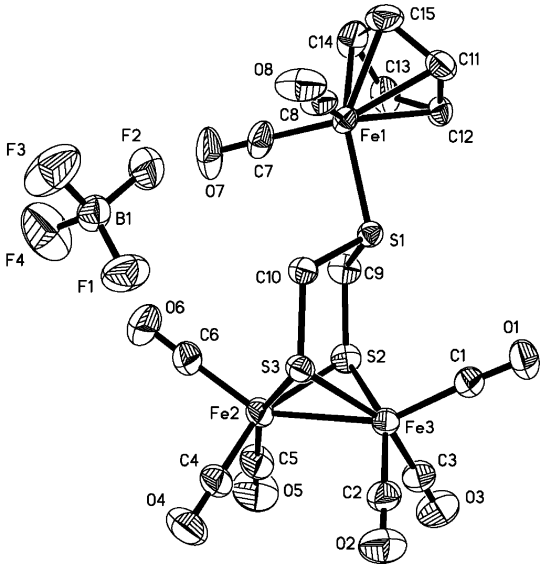

Figure 2. Molecular structure of **2** with 30% probability level ellipsoids.

Table 2. Selected Bond Lengths (Å) and Angles (deg) for 2

Fe(1)−S(1)	2.2630(9)	Fe(3)−S(3)	2.2558(10)
Fe(2)−S(3)	2.2495(10)	Fe(3)−S(2)	2.2572(11)
Fe(2)−Fe(3)	2.5246(9)	C(9)−S(1)	1.796(3)
Fe(2)−S(2)	2.2530(11)	F(1)−B(1)	1.349(5)
F(2)−B(1)−F(1)	110.6(4)	S(3)−Fe(2)−S(2)	86.81(4)
S(3)−Fe(3)−S(2)	86.56(4)	S(3)−Fe(2)−Fe(3)	56.04(3)
S(3)−Fe(3)−Fe(2)	55.80(3)	S(2)−Fe(2)−Fe(3)	56.04(3)
S(2)−Fe(3)−Fe(2)	55.88(3)	Fe(2)−S(2)−Fe(3)	68.08(4)
C(9)−S(1)−Fe(1)	105.07(12)	Fe(2)−S(3)−Fe(3)	68.16(3)

(10) Mattson, B. M.; Graham, W. A. G. *Inorg. Chem.* **1981**, *20*, 3186.
(11) Kumar, P. G. A.; Pregosin, P. S.; Vallet, M.; Bernardinelli, G.; Jazzar, R. F.; Viton, F.; Kündig, E. P. *Organometallics* **2004**, *23*, 5410.

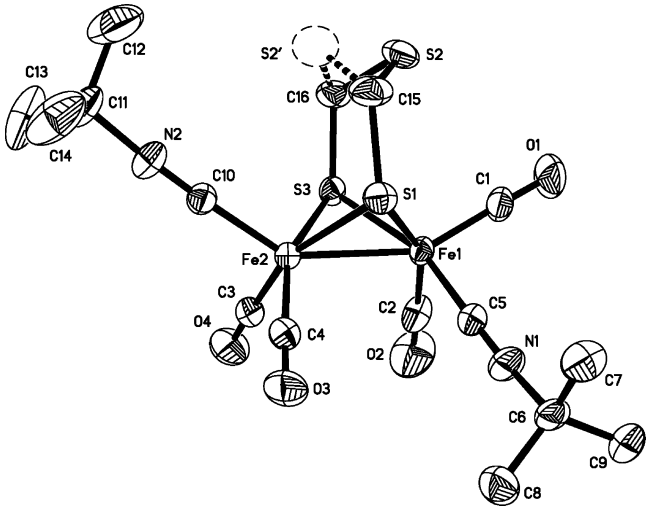

Figure 3. Molecular structure of **4** with 30% probability level ellipsoids.

Table 3. Selected Bond Lengths (Å) and Angles (deg) for 4

Fe(1)−C(5)	1.847(4)	Fe(2)−S(1)	2.2599(13)
Fe(1)−S(3)	2.2480(11)	Fe(2)−S(3)	2.2625(12)
Fe(1)−Fe(2)	2.5113(10)	C(5)−N(1)	1.153(5)
Fe(1)−S(1)	2.2589(13)	C(15)−S(2)	1.762(5)
C(15)−S(2)−C(16)	99.5(2)	S(1)−Fe(2)−Fe(1)	56.22(3)
C(5)−Fe(1)−Fe(2)	104.11(13)	S(3)−Fe(2)−Fe(1)	55.89(3)
S(3)−Fe(1)−Fe(2)	56.44(3)	C(5)−N(1)−C(6)	171.9(4)
S(1)−Fe(1)−Fe(2)	56.26(4)	N(1)−C(5)−Fe(1)	178.5(4)

steric repulsion of the axially bonded carbonyl ligand with the bulky axially bonded $Cp(CO)_2Fe$ moiety.

The TDT-type dicyanide model $(Et_4N)_2[Fe_2(\mu\text{-}SCH_2)_2S(CO)_4(CN)_2]$ (**3**) could be prepared by treatment of **1** with 2 equiv of Et_4NCN in MeCN from 0 °C to room temperature in 93% yield, but the corresponding bis(isonitrile) model $Fe_2(\mu\text{-}SCH_2)_2S(CO)_4(t\text{-BuNC})_2$ (**4**) was obtained by reaction of **1** with ca. 2 equiv of *t*-BuNC in CH_2Cl_2 at room temperature in 51% yield (Scheme 1). While **3** is a very air-sensitive and highly hygroscopic solid, **4** is much less air-sensitive both in the solid state and in solution. The spectroscopic data of **3** and **4** are consistent with their structures. For example, the IR spectra of **3** and **4** exhibit three or four absorption bands in the region 2003−1887 cm^{-1}, which are shifted to lower frequencies relative to those of the parent compound **1**, owing to the increased π-back-bonding by displacement of CO with much stronger electron-donating ligands CN^- and *t*-BuNC. The IR spectra of **3** and **4** also display a strong absorption band at 2075 cm^{-1} for the cyanide ligand in **3** or at 2143 cm^{-1} for the isonitrile ligand in **4**, respectively. The ^1H NMR spectrum of **3** or **4**, similar to that of parent compound **1**, shows a singlet at ca. 3.2 ppm at room temperature for their CH_2 groups attached to the S atoms. This implies that the interconversion between the two fused six-memberd rings in the TDT-bridged diiron system of **3** or **4** is fast enough not to permit distinguishing the two diastereotopic hydrogen atoms in their CH_2 groups at this temperature.

The X-ray diffraction analysis of **4** (Figure 3 and Table 3) has indicated that one isonitrile ligand is apically bonded to one of the square pyramidal Fe atoms and the other isonitrile ligand is basally bound to the other square pyramidal Fe atom. This kind of apical/basal (abbreviated as a/b) isomer for the TDT-type model **4** is different from the a/a isomer of the corresponding PDT-type model $Fe_2(\mu\text{-}SCH_2)_2CH_2(CO)_4(t\text{-BuNC})_2$, in which both isonitrile ligands occupy the two apical positions of the square pyramidal Fe atoms.[7b] Interestingly, **4** crystallized in two conformers: in the dominant (88%) conformer the middle sulfur (namely, S2) points opposite the apically substituted *t*-BuNC, while in the minor conformer (12%) the middle sulfur atom (S2′) points opposite the basally substituted *t*-BuNC. Apparently, such a conformer distribution is consistent with the former having much less steric repulsion between the middle sulfur atom and the apically bonded bulky *t*-BuNC ligand.

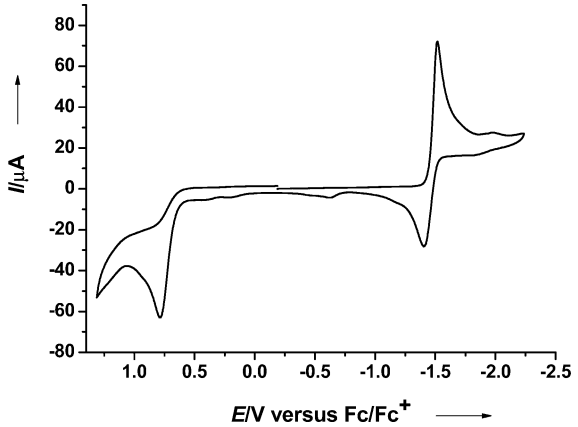

Figure 4. Cyclic voltammogram of **1** (1.0 mM) in 0.1 M $n\text{-}Bu_4NPF_6$/MeCN at a scan rate of 100 mV s^{-1}.

Electrochemistry of Parent Model 1. The electrochemical behavior of **1** was investigated by CV techniques. The cyclic voltammogram of **1** (Figure 4) displays a quasi-reversible one-electron reduction process at $E_{pc} = -1.51$ V, an irreversible one-electron reduction process at $E_{pc} = -1.94$ V, and an irreversible one-electron oxidation process at $E_{pa} = +0.79$ V. The first reduction process can be assigned to the reduction of Fe^IFe^I to Fe^IFe^0, the second reduction process to the reduction of Fe^IFe^0 to Fe^0Fe^0, and the oxidation process to the oxidation of Fe^IFe^I to Fe^IFe^{II}. The presence of a one-electron reduction process at −1.51 V or a one-electron oxidation process at +0.79 V was confirmed by bulk electrolysis of a CO-saturated acetonitrile solution of **1** at −1.75 V (50 min) or at +1.00 V (1 h). It follows that such cyclic voltammetric behavior is very similar to that of its ODT and PDT analogues $Fe_2(\mu\text{-}SCH_2)_2O(CO)_6$[6b] and $Fe_2(\mu\text{-}SCH_2)_2CH_2(CO)_6$.[8b] Recently, Pickett and coworkers have indicated that electrochemical reduction of $Fe_2(\mu\text{-}SCH_2)_2CH_2(CO)_6$ in a CO-saturated MeCN solution with some degassed water leads initially to a short-lived one-electron-reduced intermediate, $[Fe_2(\mu\text{-}SCH_2)_2CH_2(CO)_6]^-$, and then to the two-electron-reduced μ-CO-containing product $[Fe_2(\mu\text{-}S(CH_2)_3SH(\mu\text{-}CO)CO)_6]^-$.[12]

Further cyclic voltammetric study has demonstrated that model **1** has the ability for proton reduction to hydrogen in the presence of a weak acid, Et_3NHCl ($pK_a = 18.7$ in MeCN). As shown in Figure 5, upon addition of the first 2 mg of Et_3NHCl to the solution of **1**, the initial first reduction peak at −1.51 V slightly increased but did not continue to grow up with sequential addition of the acid. However, in contrast to this, upon addition of the first 2 mg of the acid, the initial second reduction peak at −1.94 V markedly increased and continued to increase with increasing concentration of the acid. Such observations are characteristic of an electrocatalytic proton reduction process.[13−15]

(12) Borg, S. J.; Behrsing, T.; Best, S. P.; Razavet, M.; Liu, X.; Pickett, C. J. *J. Am. Chem. Soc.* **2004**, *126*, 16988.
(13) Mejia-Rodriguez, R.; Chong, D.; Reibenspies, J. H.; Soriaga, M. P.; Darensbourg, M. Y. *J. Am. Chem. Soc.* **2004**, *126*, 12004.
(14) Bhugun, I.; Lexa, D.; Saveant, J.-M. *J. Am. Chem. Soc.* **1996**, *118*, 3982.

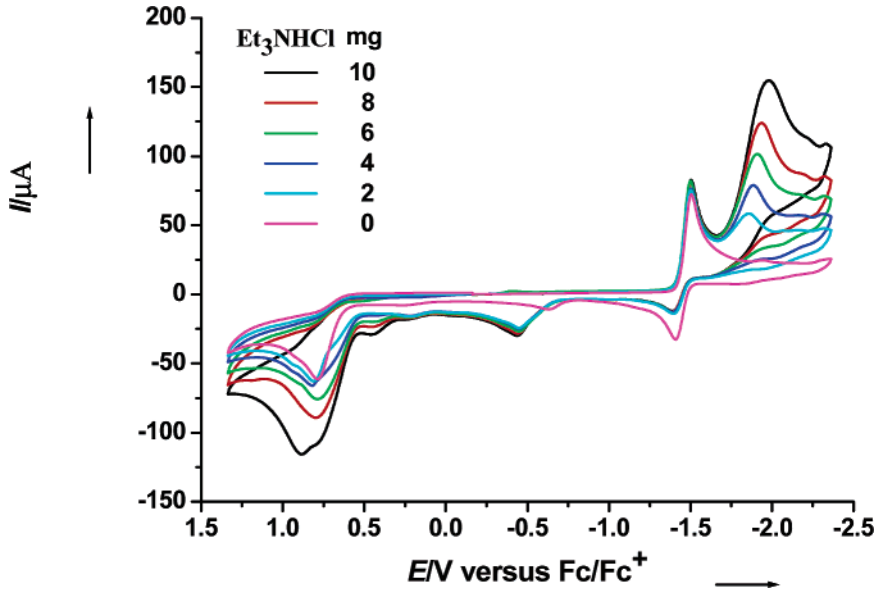

Figure 5. Cyclic voltammogram of **1** (1.0 mM) with Et_3NHCl (0−10 mg) in 0.1 M *n*-Bu_4NPF_6/MeCN at a scan rate of 100 mV s^{-1}.

The electrocatalytic activity of **1** could be further confirmed by bulk electrolysis of a MeCN solution of **1** (0.5 mM) with excess Et_3NHCl (25 mM) at −2.20 V. The total charge passed through the cell is 21 F per mol of **1** during the course of 0.5 h, which corresponds to 10.5 turnovers. Gas chromatographic analysis showed that the hydrogen yield was nearly 100%.

Conclusion

The first series of diiron TDT-type models **1**−**4** for the active site of Fe-only hydrogenases have been synthesized and structurally characterized. Among **1**−**4**, the parent model **1** was prepared by oxidative addition of 1,2,4-trithiolane to the zerovalent iron of $Fe_3(CO)_{12}$, whereas its derivatives **2**−**4** were prepared by coordination of the middle S atom of its TDT cofactor with the divalent iron of $Cp(CO)_2Fe(BF_4)$ or by displacement of its CO with cyanide and isonitrile ligands, respectively. Particularly noteworthy is that model **1** as a representative of this series has been found to have the catalytic function for proton reduction to hydrogen under electrochemical conditions. Considering the potential coordination ability of the middle S atom in the TDT cofactor[16] and the facile substitution of the Fe-bound CO by other ligands,[17] it can be expected that a great variety of such TDT-type models could be synthesized from models **1**−**4**, and thus models **1**−**4** would play an important role in the development of biomimetic chemistry of Fe-only hydrogenases.

Experimental Section

General Comments. All reactions were performed using standard Schlenk and vacuum-line techniques under N_2 atmosphere. Dichloromethane was distilled over P_2O_5 under N_2. Acetonitrile was distilled once from P_2O_5 and then freshly distilled from CaH_2 under N_2. THF was purified by distillation under N_2 from sodium/benzophenone ketyl. $AgBF_4$ and Et_4NCN were available commercially and used as received. $Fe_3(CO)_{12}$,[18] 1,2,4-trithiolane,[19] $Cp(CO)_2FeI$,[20] and *t*-BuNC[21] were prepared according to literature procedures. Preparative TLC was carried out on glass plates (26 × 20 × 0.25 cm) coated with silica gel H (10−40 μm). IR spectra were recorded on a Bruker Vector 22 infrared spectrophotometer. $^1H(^{19}F)$ NMR were recorded on a Bruker AC-P 200 NMR or a Varian Mercury Plus 400 MHz NMR spectrometer. Elemental analyses were performed on an Elementar Vario EL analyzer. Melting points were determined on a Yanaco MP-500 apparatus and are uncorrected.

Preparation of $Fe_2(\mu\text{-}SCH_2)_2S(CO)_6$ (1). A green solution of $Fe_3(CO)_{12}$ (2.016 g, 4.0 mmol) in THF (40 mL) was treated with 1,2,4-trithiolane (0.750 g, 6.0 mmol) at reflux for about 1 h. The resulting brown-red mixture was evaporated to dryness in vacuo and subjected to TLC using CH_2Cl_2/petroleum ether (1:10, v/v) as eluent. From the major red band, **1** (1.016 g, 42%) was obtained as a red solid, mp 136−137 °C. Anal. Calcd for $C_8H_4Fe_2O_6S_3$: C, 23.78; H, 1.00. Found: C, 23.62; H, 1.28. IR (KBr disk): $\nu_{C\equiv O}$ 2075 (s), 2035 (vs), 2007 (vs), 1990 (vs) cm^{-1}. ^1H NMR (200 MHz, $CDCl_3$): 3.21 (s, 4H, $2CH_2$) ppm.

Preparation of $[Fe_2(\mu\text{-}SCH_2)_2S(CO)_6][Cp(CO)_2Fe](BF_4)$ (2). A red solution of $Cp(CO)_2Fe(BF_4)$ prepared from $Cp(CO)_2FeI$ (0.076 g, 0.25 mmol) and $AgBF_4$ (0.050 g, 0.25 mmol) in CH_2Cl_2 (15 mL) was treated in situ with **1** (0.120 g, 0.30 mmol) in the dark at room temperature for 2 h. The resulting mixture was filtered to remove insoluble materials, and the filtrate was evaporated to dryness in vacuo. The residue was thoroughly washed with hexane and recrystallized by diffusion of Et_2O into its acetone solution to give **2** (0.136 g, 81%) as a red solid, mp 186 °C (dec). Anal. Calcd for $C_{15}H_9BF_4Fe_3O_8S_3$: C, 26.98; H, 1.36. Found: C, 26.95; H, 1.35. IR (KBr disk): $\nu_{C\equiv O}$ 2085 (s), 2060 (vs), 2038 (vs), 2010 (vs); ν_{B-F} 1036 (s), 1083 (s), 1123 (s) cm^{-1}. ^1H NMR (400 MHz, $(CD_3)_2CO$): 3.51 (br s, 2H, 2SC*H*H), 4.05 (br s, 2H, 2SCH*H*), 5.71 (s, 5H, C_5H_5). $^{19}F\{^1H\}$ NMR: (376 MHz, $(CD_3)_2CO$, CCl_3F): −152.09 ppm (s, BF_4).

Preparation of $(Et_4N)_2[Fe_2(\mu\text{-}SCH_2)_2S(CO)_4(CN)_2]$ (3). A solution of **1** (0.100 g, 0.25 mmol) in MeCN (15 mL) at 0 °C was

(15) Capon, J.-F.; Gloaguen, F.; Schollhammer, P.; Talarmin, J. *Coord. Chem. Rev.* **2005**, *249*, 1664.
(16) Murray, S. G.; Hartley, F. R. *Chem. Rev.* **1981**, *81*, 365.
(17) (a) Capon, J.-F.; El Hassnaoui, S.; Gloaguen, F.; Schollhammer, P.; Talarmin, J. *Organometallics* **2005**, *24*, 2020. (b) van der Vlugt, J. I.; Rauchfuss, T. B.; Wilson, S. R. *Chem.−Eur. J.* **2006**, *12*, 90.
(18) King, R. B. *Organometallic Syntheses; Transition-Metal Compounds*; Academic Press: New York, 1965; Vol. 1, p 95.
(19) Tjan, S. B.; Haakman, J. C.; Teunis, C. J.; Peer, H. G. *Tetrahedron* **1972**, *28*, 3489.
(20) King, R. B. *Organometallic Syntheses; Transition-Metal Compounds*; Academic Press: New York, 1965; Vol. 1, p 175.
(21) Gokel, G. W.; Widera, R. P.; Weber, W. P. *Organic Syntheses*; Wiley: New York, 1988; Coll. Vol. 6, p 232.

Table 4. Crystal Data and Structure Refinements for 1, 2, and 4

	1	2	4
mol formula	$C_8H_4Fe_2O_6S_3$	$C_{15}H_9BF_4Fe_3O_8S_3$	$C_{16}H_{22}Fe_2N_2O_4S_3$
mol wt	403.99	667.76	514.24
temp/K	293(2)	294(2)	293(2)
cryst syst	monoclinic	monoclinic	monoclinic
space group	*P*2(1)/*m*	P121/*c*1	*P*2(1)/*c*
a/Å	6.877(3)	21.929(6)	9.694(4)
b/Å	13.490(5)	7.5006(18)	20.457(7)
c/Å	7.975(3)	14.284(4)	12.137(4)
α/deg	90	90	90
β /deg	107.903(6)	96.078(9)	99.063(5)
γ/deg	90	90	90
V/Å^3	704.0(4)	2336.2(10)	2377.0(15)
Z	2	4	4
D_c/g cm^{-3}	1.906	1.899	1.437
abs coeff/mm^{-1}	2.519	2.177	1.505
cryst size/mm	0.28 × 0.24 × 0.20	0.20 × 0.20 × 0.20	0.38 × 0.32 × 0.24
F(000)	400	1320	1056
$2\theta_{max}$/deg	52.74	55.76	50.06
no. of reflns	4047	21 013	12 724
no. of indep reflns	1489	5526	4194
index ranges	$-8 \le h \le 6$	$-27 \le h \le 28$	$-11 \le h \le 11$
	$-16 \le k \le 16$	$-9 \le k \le 9$	$-23 \le k \le 24$
	$-9 \le l \le 9$	$-17 \le l \le 18$	$-14 \le l \le 14$
goodness of fit on F^2	1.058	1.082	1.053
R	0.0242	0.0433	0.0404
R_w	0.0538	0.1118	0.1239
largest diff peak and hole/e Å^{-3}	0.245/−0.316	0.639/−0.443	0.690/−0.427

treated with a solution of Et_4NCN (0.080 g, 0.50 mmol) in MeCN (15 mL). After the reaction mixture was warmed to room temperature, it was stirred for an additional 1.5 h. Solvent was removed in vacuo, and the residue was washed thoroughly with ether and hexane. The washed residue was further recrystallized by diffusion of Et_2O into its MeCN solution to give **3** (0.153 g, 93%) as a red solid, mp 126 °C (dec). Anal. Calcd for $C_{24}H_{44}Fe_2N_4O_4S_3$: C, 43.64; H, 6.71; N, 8.48. Found: C, 43.57; H, 6.81; N, 8.54. IR (KBr disk): $\nu_{C\equiv N}$ 2075 (s); $\nu_{C\equiv O}$ 2003 (s), 1965 (vs), 1926 (vs), 1887 (vs) cm^{-1}. ^{1}H NMR (400 MHz, $(CD_3)_2CO$): 3.43 (q, ^3J = 6.8 Hz, 16H, 8C*H*$_2$CH$_3$), 3.30 (s, 4H, 2SCH$_2$), 1.34 (t, ^3J = 6.8 Hz, 24H, 8CH$_2$C*H*$_3$) ppm.

Preparation of $Fe_2(\mu\text{-}SCH_2)_2S(CO)_4(t\text{-}BuNC)_2$ (4). To a solution of **1** (0.243 g, 0.60 mmol) in CH_2Cl_2 (20 mL) was added *t*-BuNC (0.105 g, 1.27 mmol), and then the mixture was stirred at room temperature for 20 h. The resulting brown-red mixture was evaporated to dryness in vacuo and subjected to TLC separation using CH_2Cl_2/petroleum ether (1:2, v/v) as eluent. From the main red band, **4** (0.159 g, 51%) was obtained as a red solid, mp 180 °C (dec). Anal. Calcd for $C_{16}H_{22}Fe_2N_2O_4S_3$: C, 37.37; H, 4.31; N, 5.45. Found: C, 37.21; H, 4.38; N, 5.48. IR (KBr disk): $\nu_{N\equiv C}$ 2143 (vs); $\nu_{C\equiv O}$ 2000 (vs), 1969 (vs), 1945 (vs) cm^{-1}. ^{1}H NMR (400 MHz, $(CD_3)_2CO$): 3.13 (s, 4H, 2SCH$_2$), 1.48 (s, 18H, 2C(CH$_3$)$_3$) ppm.

X-ray Structure Determinations of 1, 2, and 4. Single crystals of **1**, **2**, and **4** suitable for X-ray diffraction analyses were grown by slow evaporation of a CH_2Cl_2/petroleum ether solution of **1** at 4 °C and a CH_2Cl_2/hexane solution of **4** at −20 °C and slow diffusion of ethyl ether into an acetone solution of **2** at −20 °C, respectively. A single crystal of **1**, **2**, or **4** was mounted on a Bruker SMART 1000 automated diffractometer. Data were collected at room temperature, using a graphite monochromator with Mo Kα radiation (λ = 0.71073 Å) in the $\omega-\phi$ scanning mode. Absorption correction was performed by the SADABS program.[22] The structures were solved by direct methods using the SHELXS-97 program[23] and refined by full-matrix least-squares techniques (SHELXL-97)[24] on F^2. Hydrogen atoms were located by using the geometric method. Details of crystal data, data collections, and structure refinements are summarized in Table 4.

Electrochemistry. A solution of 0.1 M *n*-Bu_4NPF_6 in MeCN (Fisher Chemicals, HPLC grade) was used as electrolyte in all cyclic voltammetric experiments. The electrolyte solution was degassed by bubbling with dry N_2 for 10 min before measurement. Electrochemical measurements were made using a BAS Epsilon potentiostat. All voltammograms were obtained in a three-electrode cell with a 3 mm diameter glassy carbon working, platinum counter, and Ag/Ag$^+$ (0.01 M $AgNO_3$/0.1 M *n*-Bu_4NPF_6 in MeCN) reference under N_2 atmosphere. The working electrode was polished with 1 μm alumina paste and sonicated in water for 10 min prior to use. All potentials are quoted against the ferrocene/ferrocenium (Fc/Fc$^+$) potential. Bulk electrolyses for electrocatalytic reactions were carried out under a N_2 or CO atmosphere using a BAS Epsilon potentiostat. Electrocatalytic experiments were run on a glassy carbon rod (A = 2.9 cm^2) in a two-compartment, gastight, H-type electrolysis cell containing ca. 25 mL of MeCN. The electrolyses of solutions were carried out under hydrodynamic conditions, vigorously stirring the solutions, to mitigate mass transport complications. Gas chromatography was performed with a Shimadzu GC-9A gas chromatograph under isothermal conditions with nitrogen as a carrier gas and a thermal conductivity detector.

Acknowledgment. We are grateful to the National Natural Science Foundation of China and the Research Fund for the Doctoral Program of Higher Education of China for financial support.

Supporting Information Available: Full tables of crystal data, atomic coordinates, thermal parameters, and bond lengths and angles for **1**, **2**, and **4** as CIF files. This material is available free of charge via the Internet at http://pubs.acs.org.

OM061186Z

(22) Sheldrick, G. M. *SADABS, A Program for Empirical Absorption Correction of Area Detector Data*; University of Göttingen: Germany, 1996.

(23) Sheldrick, G. M. *SHELXS97, A Program for Crystal Structure Solution*; University of Göttingen: Germany, 1997.

(24) Sheldrick, G. M. *SHELXL97, A Program for Crystal Structure Refinement*; University of Göttingen: Germany, 1997.